33RD CONGRESS
OF THE INTERNATIONAL COUNCIL
OF THE AERONAUTICAL SCIENCES
STOCKHOLM, SWEDEN, 4-9 SEPTEMBER, 2022

ICAS 2022 SWEDEN

ESTIMATION OF ROTOR IMBALANCE AND MODEL DISCREPANCY USING A BAYESIAN APPROACH

Rahul Rameshbabu[1], Dushhyanth Rajaram[1], Olivia J. Pinon Fischer[1] & Dimitri N. Mavris[1]

[1]Aerospace Systems Design Laboratory (ASDL), School of Aerospace Engineering, Georgia Institute of Technology, Atlanta, GA, 30332, U.S.A

Abstract

The use of rotating machinery is prevalent in the aerospace industry. For example, rotating shafts are very common in turbines, compressors, and engines. Rotor imbalance is one of the most common faults that occurs in rotating machinery. It may lead to excessive vibrations and ultimately to the failure of components. Imbalance of a rotor is typically estimated by measuring vibration in conjuction with a physics-based model. This includes some point estimation methods to determine imbalance parameters to best match observed data. Bayesian methods have also been employed to approximate distributions of imbalance parameters to aid in uncertainty quantification. However, the aforementioned methods do not account for model discrepancy, which quantifies the missing or incorrect physics within the finite element model used to model the rotating system. Accounting for model discrepancy will result in an improved uncertainty quantification of imbalance parameters. To demonstrate this benefit, this paper proposes the application of a Bayesian method that accounts for model discrepancy to the rotor imbalance estimation problem. Compared to Bayesian approaches that do not account for discrepancy, the methodology in this paper results in imbalance estimates of similar accuracy but with more useful measures of uncertainty.

Keywords: Rotating Systems, Imbalance, Bayesian Inference, Uncertainty Quantification, Discrepancy Modeling

1. Introduction

Rotating machinery is very prevalent in the aerospace industry. For example, rotating shafts are very common in turbines, compressors, and engines. Rotor imbalance is one of the most common faults that occur in rotating machinery [1]. It alters the vibration profile of the shaft that it affects, which ultimately can cause damage or the failure of components. Due to the advent of sensor technology, such as accelerometers and proximity sensors, many research efforts have been focusing on outfitting rotating shafts with sensors, collecting data, and utilizing this data to estimate imbalance, including estimating the eccentricity and phase of the imbalance. It is expected that the proper estimation of rotor imbalance can then be used for condition-based maintenance purposes, resulting in time and cost savings. The following sections briefly discuss some of the common approaches to rotor imbalance estimation and their limitations.

1.1 Machine Learning Approaches

A number of supervised machine learning approaches have been proposed to estimate imbalance. For example, Reddy et al. [2] used neural networks to estimate rotor imbalance. Similarly, Singh et al. [3] tested neural networks and support vector machines to estimate rotor imbalance. However, these approaches have a number of issues and limitations . First, they both solve the problem of classifying vibration data into predetermined imbalance classes, which means they cannot extrapolate to unseen imbalance states. In addition, they require labeled data, which may not be available or may be difficult to obtain. There have been approaches that use a simulated system to train classifiers [4], which help with the data problem but not the extrapolation problem.

1.2 Signal Processing Approaches

Another class of methods used for imbalance estimation includes signal processing methods.In [5], Kral et al. detect imbalance using signal processing methods on power measurements of rotating systems. In [6], Caccicola et. al detect imbalance using a harmonic analysis on sensor measurements. In [7], Yamamoto et al. use an fast Fourier transform (FFT) on a time domain vibration signal along with an FPGA setup to detect and correct rotor imbalance. Unlike the supervised learning approaches, the signal processing approaches perform well when detecting the presence of imbalance without the need for labels. However, compared to model-based approaches, they perform poorly when estimating the imbalance eccentricity and phase [8].

1.3 Model-based Approaches

Multiple model-based methods have been proposed and leveraged for imbalance estimation that make use of both vibration measurements and physics-based models. Market et al. [9], Sudhakar et al. [8], Shrivastava et al. [10], and Abbasi et al. [11], for example, describe approaches that estimate rotor imbalance by utilizing physics-based rotor models and vibration measurements using least-squares approaches. In [12], Zou et al., estimate imbalance parameters using a Kalman filtering approach. In [13], Yao et al. utilize a model-based inverse problem approach to solve the imbalance estimation problem. In [14], Wang et al. use a model-based method to estimate imbalance parameters using equations derived in the frequency domain. The aforementioned approaches allow for both accurate detection of imbalance along with more accurate estimation of the eccentricity and phase of the imbalance. However, these approaches tend to provide only point estimates of imbalance parameters, and do not inform about the uncertainty of the estimates. However, multiple sources of uncertainty exist when estimating imbalance in rotating systems that need to be captured and estimated.

1.4 Bayesian Approaches

In rotating systems, uncertainty exists both in the measurements and in the model parameters. In addition, when rotor models are used, there exists uncertainty in the model form, which represents the difference between the model and the true process it is representing. Due to these various sources of uncertainty, when estimating imbalance parameters, it is more appropriate to quantify the uncertainty of the parameters rather than provide point estimates. Often times, prior knowledge, either weak or specific, is known about the parameters of interest. Consequently, it is common to use Bayesian inference to learn posterior distributions of parameters given prior information in the form of prior distributions, and data in the form of a likelihood distribution. From there, the posterior distribution can be analyzed to obtain the expected value of the imbalance parameters along with uncertainty. In [1, 15], Garoli et al. use a method involving polynomial chaos expansion to efficiently approximate the posterior distributions of imbalance parameters. In [16], Tyminski et al. use a Markov Chain Monte Carlo (MCMC) algorithm to approximate the distributions. In [17], Taherkhani et al. also uses MCMC to infer imbalance parameters among others selected through sensitivity analysis for a rotating system. In [18], Corbalan et. al use MCMC along with current measurements to estimate imbalance parameters. While these approaches account for the uncertainty in both model parameters and measurements, they do not account for uncertainty of the model form, also known as the model discrepancy.

Model discrepancy arises because a model can never perfectly replicate a physical process. For this reason, model discrepancy is often learned along-side model parameters [19, 20]. Vankov et al. [21] shows that learning model discrepancy along with model parameters will improve the uncertainty quantification of parameters in the context of Bayesian parameter estimation. The scale of the improvement depends on the quality of the prior information for both the parameters to be estimated and the discrepancy model. With no discrepancy modeling and weak prior information, the parameter estimates are likely to be biased and have a low variance. This combination is undesirable because it can be interpreted as extremely high confidence about incorrect parameter values. With discrepancy modeling included and weak prior information, the parameter estimates are likely to be biased, but with a high variance. This result is more desirable than the case where discrepancy is not modeled.

The reason is that even though the expectation is still biased, the high variance will reflect low confidence on the expected parameter values. Finally, with discrepancy modeling combined with more informative prior information, the parameter estimates are likely to have low bias and low variance, which is the most desirable outcome.

This paper proposes to improve upon the aforementioned attempts at the rotor imbalance estimation problem. Similar to the work discussed in [1] and [16], the present research employs a model-based approach that uses Bayesian inference to provide posterior distributions of imbalance parameters given vibration data. However, when compared to existing approaches, this research accounts for model discrepancy as a means to improve the accuracy of the imbalance estimates.
The remaining of the paper is organized as follows. Section II presents some background on rotor modeling and imbalance estimation. Section III introduces the proposed methodology and Section IV discusses its implementation and results on a simulated test case. Finally, Section V summarizes the benefits of the proposed approach and discusses avenues for future work.

2. Background

This section provide relevant background on rotor modeling as well as different model-based imbalance estimation techniques.

2.1 Rotor Modeling

Equation 1 relates the vibrations of the rotor system to the force induced by an imbalance and is therefore commonly used to model rotating systems with imbalance [9].

$$M\ddot{r}(t) + B\dot{r}(t) + Kr(t) = F_0(t) + F(\beta, t) \tag{1}$$

where, $\ddot{r}(t)$, $\dot{r}(t)$, and $r(t)$ are the accelerations, velocities, and displacements of the rotor system, respectively. The M, B, and K matrices are the mass, damping/gyroscopic, and stiffness matrices respectively. $F_0(t)$ is the load acting on the rotor during nominal operation (without imbalance), and $F(\beta, t)$ is the operational load induced by imbalance in the rotor. This equation is then commonly solved using finite element methods [8].
A commonly used imbalance fault model is shown in Equations 2 and 3.

$$\Delta F_h(\beta, t) = u \sin(\omega t + \phi) \tag{2}$$

$$\Delta F_v(\beta, t) = u \cos(\omega t + \phi) \tag{3}$$

where, $\beta = [u, \phi]$ is the vector containing the imbalance parameters that we wish to estimate, u is the magnitude of the force induced by the imbalance in Newtons, and ϕ is the phase of the force induced by the imbalance in radians.
While Equations 1, 2, and 3 are in the time domain, vibration signals are often analyzed in the frequency domain. The methods employed in this paper use the frequency response of vibration signals of the rotor system. The vibration signal $r(t)$ has the frequency response, $q(\omega)$.

2.2 Imbalance Estimation

This section discusses a number of model-based imbalance estimation techniques. All the techniques described in this section make use of rotor models of the form in Equation 1 along with vibration measurements. First, least-squares approaches are presented. Second, Bayesian methods are presented.

2.2.1 Least-Squares Methods

Many implementations formulate the imbalance estimation problem as a least-squares problem. For example, [8,9] optimize imbalance parameters by choosing β to minimize Equation 4, which quantifies the difference between the force calculated by the fault model and the force calculated using the measured vibrations.

$$\sum_i |F(\beta, t_i) - F_M(t_i)|^2 \tag{4}$$

Another least-squares approach consists in choosing β to minimize the difference between the vibrations calculated by the rotor model and the measured vibrations. This can also be done by minimizing the difference between the frequency responses of both the measured and calculated vibrations, as shown in Equation 5. In Equations 4 and 5, i represents the i-th measured observation.

$$\sum_i |q(\beta, \omega_i) - q_M(\omega_i)|^2 \tag{5}$$

However, as mentioned in the introduction, the result of these least-squares methods are point estimates of imbalance, which do not account for uncertainty in measurements, model parameters, or model form.

2.2.2 Bayesian Methods

As discussed, Bayesian methods have also been implemented to estimate rotor imbalance [1,15–18]. The two methods presented in the previous sections result in point estimates of β that minimize Equations 4 and 5. In a Bayesian approach, the result is either a computation or approximation of the posterior distributions of imbalance parameters given vibration data. Unlike a point estimate, a distribution allows for the natural quantification and propagation of uncertainty. The posterior distributions are either computed or approximated using Bayes theorem, which is shown in Equation 6. This process is known as Bayesian inference.

$$\pi(\beta|q_{obs}) = \frac{L(q_{obs}|\beta)\pi(\beta)}{\pi(q_{obs})} \tag{6}$$

where, $q_{obs} = (q(\omega_1), q(\omega_2), \ldots, q_n(\omega_n))$ is the frequency response of the rotor system computed from the measured vibration signals, $\pi(\beta|q_{obs})$ is the posterior distribution of the imbalance parameters given the frequency response of the system, $L(q_{obs}|\beta)$ is the likelihood function, which is the joint density of the frequency response given the imbalance parameters and $\pi(\beta)$ is the prior distribution of the imbalance parameters.

Estimating rotor imbalance using a Bayesian approach can be accomplished by assuming the following statistical formulation.

$$q_{obs}(\omega) = q(\beta^*, \omega) + \varepsilon \tag{7}$$

where, $\beta^* = [u^*, \phi^*]$ is the vector of true imbalance parameters, and ε is the measurement error. In addition, if we assume that $\varepsilon \sim N(0, \sigma^2)$, then we can form the following likelihood function.

$$L(q_{obs}|\beta) \propto exp\left\{ -\frac{1}{2}\sigma^2 ||q_{obs} - q(\beta)||_2^2 \right\} \tag{8}$$

where, $q(\beta) = (q(\beta, \omega_1), q(\beta, \omega_2), \ldots, q(\beta, \omega_n))$ is the frequency response of the vibrations calculated using Equation 1 given β. Then assuming some prior distribution, Bayes theorem can be used to obtain an expression for the posterior distribution. This expression is shown in Equation 9.

$$\pi(\beta|q_{obs}) \propto L(q_{obs}|\beta)\pi(\beta) = exp\left\{ -\frac{1}{2}\sigma^2 ||q_{obs} - q(\beta)||_2^2 \right\} \pi(\beta) \tag{9}$$

Because the posterior distribution in Equation 9 often cannot be determined analytically, Markov Chain Monte Carlo (MCMC) methods are commonly used to sample from the posterior distribution, as discussed in [1, 16]. The expected value of the posterior can be used to represent the imbalance parameter estimates, with the uncertainty represented by the variance of the posterior.

When compared to least-squares methods, Bayesian approaches have the added benefit of uncertainty quantification and the inclusion of prior knowledge through specification of prior distributions. However, the implementations referenced in this section do not account for model discrepancy. This shortcoming is addressed in the following section.

3. Proposed Methodology

As discussed in the introduction, the main contribution of this work is to improve upon Bayesian approaches to imbalance estimation and uncertainty quantification by accounting for model discrepancy. Many efforts in fields other than rotor imbalance modeling have implemented Bayesian parameter estimation, while accounting for model discrepancy [19–23]. Inspired by these works, a statistical model that represents a rotating system with imbalance is shown in Equation 10. This Equation can be understood as Equation 7 with the addition of a discrepancy term, $\delta(\omega)$.

$$q_{obs}(\omega) = q(\beta^*, \omega) + \delta(\omega) + \varepsilon \tag{10}$$

A common method to model the discrepancy function is to use a Gaussian Process (GP) as shown in Equations 11 and 12. The Bayesian framework can then be used to estimate both β and the hyper-parameters of the GP.

$$\delta(\omega) \sim GP(0, k(\omega, \omega^{'})) \tag{11}$$

$$k(\omega, \omega^{'}) = \exp\left\{ -\frac{|\omega - \omega^{'}|^2}{2l^2} \right\} \tag{12}$$

In Equation 12, the hyperparameter to be estimated is l. l is the length scale of the model, which determines how quickly the discrepancy can change with respect to frequency, ω.
Given the statistical formulation in Equation 10 and that $\delta(\omega)$ is a GP with zero mean and covariance function of the form in Equation 12, an expression for the likelihood function, $L(q_{obs}|\beta, l)$, can be derived, as shown in equation 13.

$$L(q_{obs}|\beta, l) \propto exp\left\{ -\frac{1}{2}(q_{obs} - q(\beta))^T \Sigma (q_{obs} - q(\beta)) \right\} \tag{13}$$

$$\Sigma = \Sigma_\varepsilon + \Sigma_\delta \tag{14}$$

In Equation 14, Σ_δ is the matrix formed by applying Equation 12 to all the frequency values considered, and Σ_ε is assumed to be known. Next, given the likelihood function and prior distributions, Equation 15 can be used to represent the posterior distribution of the imbalance parameters and the discrepancy model hyperparameter given the frequency response of the vibration measurements.

$$\pi(\beta, l|q_{obs}) \propto L(q_{obs}|\beta, l)\pi(\beta)\pi(l) = exp\left\{ -\frac{1}{2}(q_{obs} - q(\beta))^T \Sigma (q_{obs} - q(\beta)) \right\} \pi(\beta)\pi(l) \tag{15}$$

In Equation 15, $\pi(\beta)$ and $\pi(l)$ are the prior distributions of the imbalance parameters and discrepancy model hyperparameter. As described earlier, MCMC can be used to sample from the posterior distributions of these parameters, and the expected value of the posterior can be used to represent the imbalance parameter estimates, with the uncertainty represented by the variance of the posterior.

4. Implementation and Results

4.1 Rotor Models

The rotor models used in this paper were implemented using the ROSS python library [24]. This library allows the user to define a rotor system consisting of various components such as shaft elements, bearings, and disks. Then the system is discretized into nodes via the finite element method, which results in Equation 1.
Two different rotor models were configured. Both rotor models consist of one disk and two support bearings on a shaft, as shown in Figure 1. The first rotor model represents a real system. It is of interest to estimate the imbalance of the disk for this model. Throughout the rest of the paper, this model will be referred to as the real model. The second model represents a simulation model used to estimate the imbalance of the real model. Throughout the rest of the paper, this model will be referred to as the simulation model. The shaft and disk properties are summarized in Table 1, and the bearing properties are summarized in Table 2.

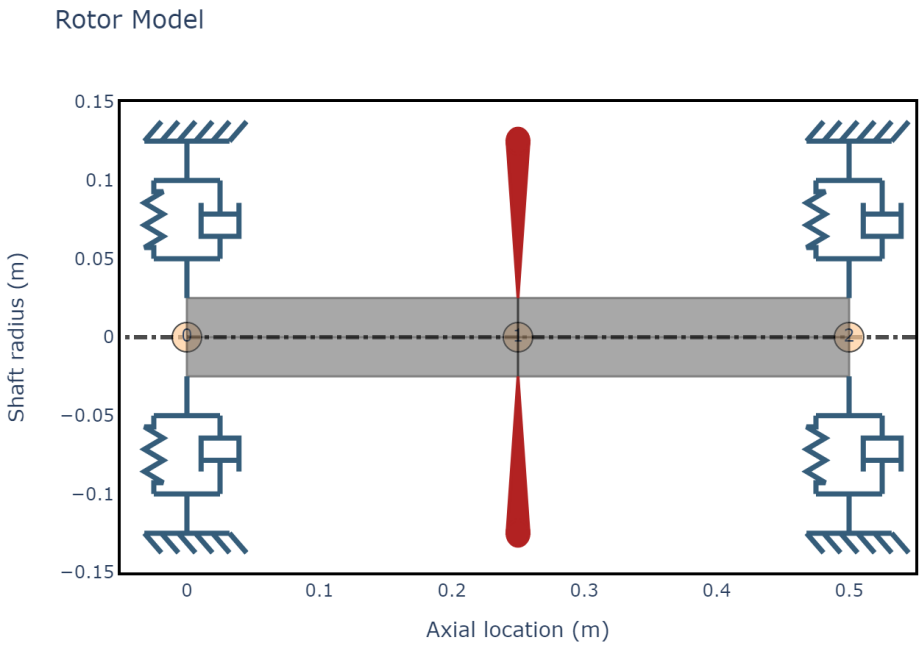

Figure 1 – Rotor Diagram

As shown in Table 2, to simulate model discrepancy through missing physics, the bearings on the real model impart damping into the system, while the bearings on the simulated model impart no damping into the system. The shaft properties are identical for both real and simulation models.

component	Length (m)	inner diameter (m)	outer diameter (m)	material
shaft	0.5	0.0	0.05	Steel
disk	0.07	0.05	0.28	Steel

Table 1 – Shaft and Disk Characteristics

component	x stiffness (N/m)	y stiffness (N/m)	x damping (Ns/m)	y damping (Ns/m)
real bearings	1e6	0.8e6	3e3	3e3
simulation bearings	1e6	0.8e6	0	0

Table 2 – Bearing Characteristics

The imbalance force applied to the disk was of magnitude 0.03 Newton and phase 0 radian. The frequency response of this imbalance applied to the real model is shown in Figure 2, and for the simulation model in Figure 3. The frequency response displayed in both of the figures is the frequency response of the imbalanced system in the x direction.
The differences between the frequency responses of the real and simulation models are due to the damping effects present in the real model, but not present in the simulation model. Only the x component frequency responses are shown because they are good enough to show the effect of the missing physics. However, both x and y directions of the frequency response are considered when estimating the imbalance parameters. The frequency range considered was 61 evenly spaced discrete frequencies between 315 and 1155 radians per second. Due to time constraints, 61 was chosen as the number of sample points. While more points could have been generated, this would have considerably increased the computational time due to the increased dimensionality of the Gaussian Process

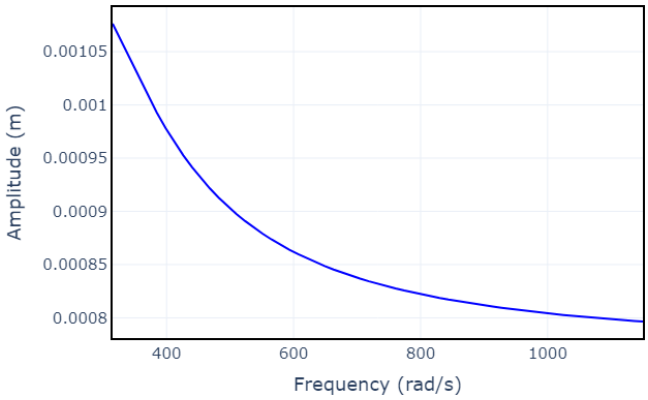

(a) Magnitude

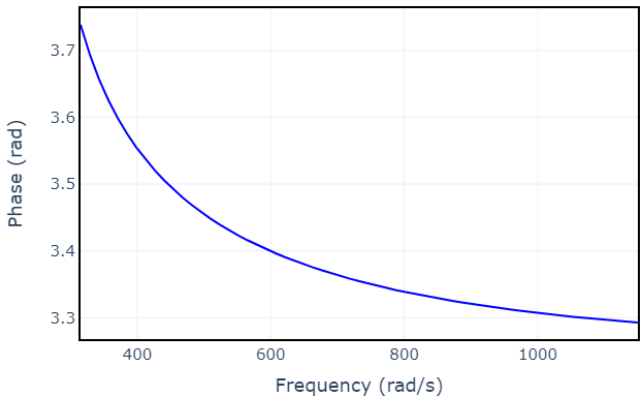

(b) Phase

Figure 2 – Frequency Response of Real Model (x direction)

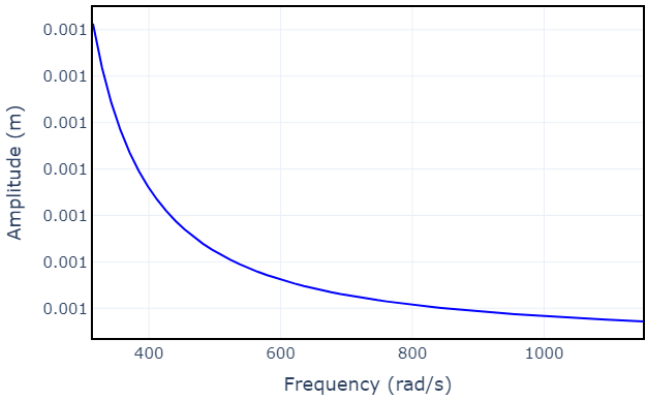

(a) Magnitude

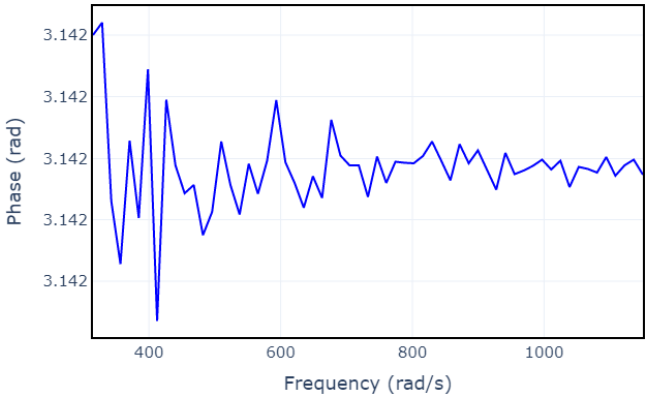

(b) Phase

Figure 3 – Frequency Response of Simulation Model (x direction)

covariance matrices. Also, since the purpose of this paper is to study the effect of model discrepancy and not measurement error, the measurement error was chosen to be negligible.

4.2 Estimation Methods

Two Bayesian imbalance estimation methods are compared as part of this research. The first calculates the posterior distribution of the disk imbalance using Bayesian inference without accounting for model discrepancy, as shown in Equation 9. This method will be referred to as the baseline method. The second calculates the posterior distribution of the disk imbalance using Bayesian inference while accounting for model discrepancy in the form of a GP, as shown in Equation 15. This method will be referred to as the discrepancy method. Prior distributions were chosen for the imbalance parameters to represent a realistic scenario in which imbalance parameters are to be estimated. This means having a general idea about the magnitude and range of the imbalance parameters, but not knowing the values to a high degree of certainty. The prior distributions for relevant parameters are shown in Table 3.

parameter	prior distribution
u	$HalfNormal(\mu = 0, \sigma = 0.05)$
ϕ	$Uniform(lower = 0, upper = \pi)$
l	$Gamma(\alpha = 5, \beta = 5)$ (bounded above by 4)

Table 3 – Prior Distributions

The half-normal prior was chosen for the imbalance magnitude, u, because it has non-negative support. Zero mean and a small variance were chosen to represent a situation in which it is known that the imbalance magnitude is likely small. A uniform prior was chosen for the imbalance phase to represent a situation where no prior knowledge is known about the imbalance phase except for the obvious fact that it is an angle. Finally a bounded Gamma distribution was chosen for the lengthscale of the GP, l. A gamma distribution was chosen because we may be interested in large positive values. However, it is bounded at 4, to not allow lengthscales that are too large.
For both the baseline and discrepancy methods, the Metropolis Hastings MCMC algorithm was chosen to approximate the posterior distributions [25]. The MCMC algorithm was implemented using the PyMC3 Python library [26].

4.3 Results

The baseline and discrepancy methods were employed to estimate the imbalance of the real model. The posterior distributions of the imbalance parameters from the baseline method are shown in Figure 4. The posterior distributions of the imbalance parameters and discrepancy GP length-scale from the discrepancy method are shown in Figure 5. For both approaches, four separate chains were sampled with 2000 tuning samples and 1000 draw samples for each chain.
In the figures above, each plot shows the posterior samples resulting from the MCMC sampling for each parameter. The magnitude plots indicate that the expectation of the half-normal prior shifts from zero to a value closer to the ground-truth magnitude for both baseline and discrepancy methods. Similarly, for the phase plots, the expectation of the uniform prior shifts from $\frac{\pi}{2}$ to a value much closer to the true phase for both the baseline and discrepancy approaches. The posterior plot of the length-scale does not provide direct information about the imbalance parameters, but the fact that the length-scale samples have converged indicates that the number of MCMC iterations are sufficient.
The mean and variance of the posterior distributions for both methods are summarized in Table 4.
To quantify the effectiveness of both imbalance estimation methods, the absolute value of the true errors of the posterior means with respect to the ground truth imbalance parameters are calculated. These results are shown in Table 5
From the results in Table 5, it seems that both methods appear very comparable in terms of estimation error. However, the advantage of accounting for model discrepancy is more apparent when considering uncertainty quantification. As shown in Table 4, while the means of the posterior distributions are

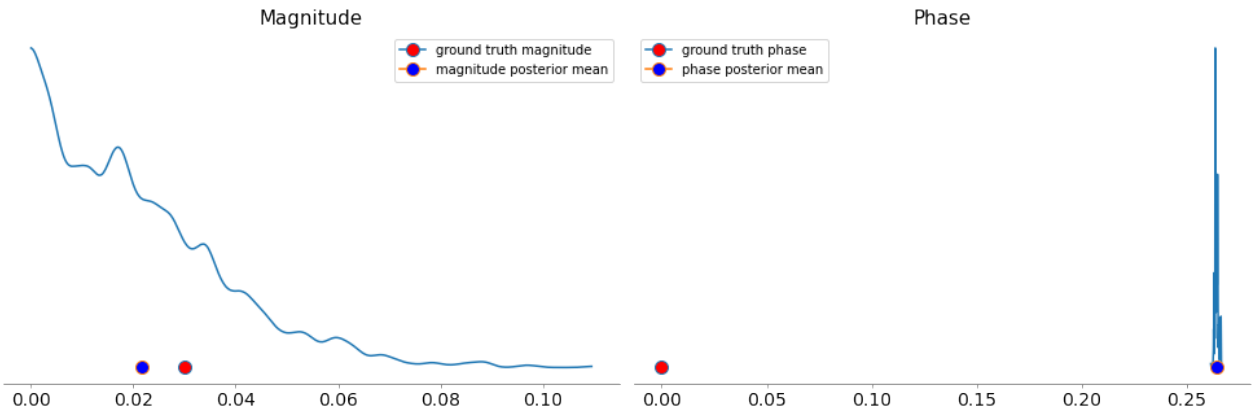

Figure 4 – Posterior Distributions, no Discrepancy

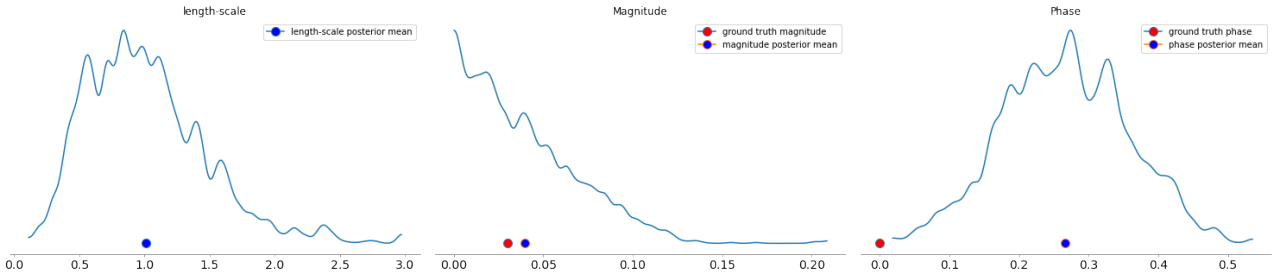

Figure 5 – Posterior Distributions, with Discrepancy

similar for both approaches, the standard deviation of the posterior distributions are quite different. Specifically, the standard deviations of the posteriors from the discrepancy method are quite larger. This can be seen in posterior plots in Figures 4 and 5, especially for the phase. The conclusion from this is that, while both methods produce estimates with some bias, the discrepancy method is not overconfident about the biased estimates, unlike the baseline method, which is extremely confident about the biased estimates due to the uncertainty resulting from model discrepancy not being included. Being extremely confident about incorrect estimates is not desirable when making potentially costly maintenance decisions. On the contrary, due to accounting for model discrepancy alongside the forms of uncertainty already considered, then a practitioner can make a better judgement call on whether or not to enact maintenance when using the discrepancy method.

5. Concluding Remarks

In this paper, two Bayesian approaches were tested on the Rotor Imbalance Estimation problem. The first method calculated posterior distributions of the imbalance parameters without accounting for model discrepancy. This was the baseline method. The second method calculated posterior distributions of the imbalance parameters, while accounting for model discrepancy. Both methods exhibited similar levels of bias when comparing the expected value of the posteriors to the true imbalance parameters. However, the variance of the posteriors from the baseline method signified extreme confidence about these biased estimates. The discrepancy method did not posses this undesirable quality. In conclusion, these results motivate further exploration of discrepancy modeling in Bayesian imbalance estimation. In particular, future work could include investigating more specific prior information for the discrepancy models to lower the bias of imbalance estimates. This could include adding constraints to the Gaussian Process discrepancy model based on prior knowledge of characteristics specific to rotor systems.

6. Contact Author Email and Phone

Olivia J. Pinon Fischer: olivia.pinon@asdl.gatech.edu

Method	Parameter	Mean	Standard Deviation
baseline	u	0.0216	0.0171
baseline	ϕ	0.2642	0.0008
discrepancy	u	0.0396	0.0306
discrepancy	ϕ	0.2662	0.0895
discrepancy	l	1.0083	0.4547

Table 4 – Posterior Distribution Statistics

Method	magnitude error	phase error
baseline	0.0084	0.2642
discrepancy	0.0096	0.2662

Table 5 – Method Benchmarking

7. Copyright Statement

References

[1] Gabriel Yuji Garoli, Diogo Stuani Alves, Tiago Henrique Machado, Katia Lucchesi Cavalca, and Helio Fiori de Castro. Fault parameter identification in rotating system: Comparison between deterministic and stochastic approaches. *Structural Health Monitoring*, 20(6):3182–3200, 2021.

[2] M Chandra Sekhar Reddy, AS Sekhar, et al. Application of artificial neural networks for identification of unbalance and looseness in rotor bearing systems. *International Journal of Applied Science and Engineering*, 11(1):69–84, 2013.

[3] Sukhjeet Singh and Navin Kumar. Rotor faults diagnosis using artificial neural networks and support vector machines. *International Journal of Acoustics and Vibration*, 20(3):153–159, 2015.

[4] TG Ritto and FA Rochinha. Digital twin, physics-based model, and machine learning applied to damage detection in structures. *Mechanical Systems and Signal Processing*, 155:107614, 2021.

[5] C. Kral, T.G. Habetler, and R.G. Harley. Detection of mechanical imbalances of induction machines without spectral analysis of time-domain signals. *IEEE Transactions on Industry Applications*, 40(4):1101–1106, 2004.

[6] S. Cacciola, I. Munduate Agud, and C.L. Bottasso. Detection of rotor imbalance, including root cause, severity and location. *Journal of Physics: Conference Series*, 753:072003, sep 2016.

[7] Guilherme Kenji Yamamoto, Cesar da Costa, and João Sinohara da Silva Sousa. A smart experimental setup for vibration measurement and imbalance fault detection in rotating machinery. *Case Studies in Mechanical Systems and Signal Processing*, 4:8–18, 2016.

[8] G. N. D. S. Sudhakar and A. S. Sekhar. Identification of unbalance in a rotor bearing system. *Journal of Sound Vibration*, 330(10):2299–2313, May 2011.

[9] Richard Markert, Roland Platz, and Malte Seidler. Model based fault identification in rotor systems by least squares fitting. *International Journal of Rotating Machinery*, 7(5):311–321, 2001.

[10] Akash Shrivastava and Amiya R Mohanty. Identification of unbalance in a rotor-bearing system using kalman filter–based input estimation technique. *Journal of Vibration and Control*, 26(11-12):1081–1091, 2020.

[11] Ahmad Abbasi, Behnam Firouzi, Polat Sendur, Gyan Ranjan, and Rajiv Tiwari. Identification of unbalance characteristics of rotating machinery using a novel optimization-based methodology. 26(10), 2022.

[12] Donglin Zou, Han Zhao, Gaoyu Liu, Na Ta, and Zhushi Rao. Application of augmented kalman filter to

identify unbalance load of rotor-bearing system: Theory and experiment. *Journal of Sound and Vibration*, 463:114972, 2019.

[13] Jianfei Yao, Liang Liu, Fengyu Yang, Fabrizio Scarpa, and Jinji Gao. Identification and optimization of unbalance parameters in rotor-bearing systems. *Journal of Sound and Vibration*, 431:54–69, 2018.

[14] Aiming Wang, Yujie Bi, Yu Feng, Jie Yang, Xiaohan Cheng, and Guoying Meng. Continuous rotor dynamics of multi-disc and multi-span rotors: A theoretical and numerical investigation of the identification of rotor unbalance from unbalance responses. *Applied Sciences*, 12(8), 2022.

[15] Gabriel Y. Garoli, Rafael Pilotto, Rainer Nordmann, and Helio F. de Castro. Identification of active magnetic bearing parameters in a rotor machine using bayesian inference with generalized polynomial chaos expansion. *Journal of the Brazilian Society of Mechanical Sciences and Engineering*, 43(12):552, Nov 2021.

[16] Natalia Cezaro Tyminski and Helio Fiori de Castro. Application of bayesian inference to unbalance identification in rotors. In *Proceedings of the 9th IFToMM international conference on rotor dynamics*, pages 711–721. Springer, 2015.

[17] Zahra Taherkhani and Hamid Ahmadian. Stochastic model updating of rotor support parameters using bayesian approach. *Mechanical Systems and Signal Processing*, 158:107702, 2021.

[18] Patricio Corbalan and Luciano E Chiang. Rotor unbalance fault diagnosis in wind turbine by markov chain monte carlo method. 2021.

[19] Dave Higdon, Marc Kennedy, James C Cavendish, John A Cafeo, and Robert D Ryne. Combining field data and computer simulations for calibration and prediction. *SIAM Journal on Scientific Computing*, 26(2):448–466, 2004.

[20] Marc C Kennedy and Anthony O'Hagan. Bayesian calibration of computer models. *Journal of the Royal Statistical Society: Series B (Statistical Methodology)*, 63(3):425–464, 2001.

[21] Iskren Vankov, Daniel Mills, Daniela Calvetti, Jari P Kaipio, Aaron E Tallman, and Laura P Swiler. Learning about physical parameters : the importance of model discrepancy Learning about physical parameters : the importance of model discrepancy. 2014.

[22] Adrian Chong and Kathrin Menberg. Guidelines for the bayesian calibration of building energy models. *Energy and Buildings*, 174:527–547, 2018.

[23] Rebecca Ward, Ruchi Choudhary, Alastair Gregory, Melanie Jans-Singh, and Mark Girolami. Continuous calibration of a digital twin: comparison of particle filter and Bayesian calibration approaches. nov 2020.

[24] Raphael Timbó, Rodrigo Martins, Gabriel Bachmann, Flavio Rangel, Júlia Mota, Juliana Valério, and Thiago Ritto. ROSS - Rotordynamic Open Source Software. *Journal of Open Source Software*, 5(48):2120, 2020.

[25] Siddhartha Chib and Edward Greenberg. Understanding the metropolis-hastings algorithm. *The american statistician*, 49(4):327–335, 1995.

[26] John Salvatier, Thomas V Wiecki, and Christopher Fonnesbeck. Probabilistic programming in python using pymc3. *PeerJ Computer Science*, 2:e55, 2016.